

A long-time-step method for quantum-classical molecular dynamics

Tobias Jahnke

Freie Universität Berlin, Institut für Mathematik II, BioComputing Group, Arnimallee 2-6, D-14195 Berlin, Germany, e-mail: Tobias.Jahnke@math.fu-berlin.de.

The date of receipt and acceptance will be inserted by the editor

Summary A well-known quantum-classical model for molecular dynamics is investigated from a numerical point of view. In this model a classical Newtonian equation of motion is coupled to a Schrödinger equation in order to describe the quantum behaviour of the electrons. This makes an efficient numerical treatment difficult because the oscillating solution of the Schrödinger equation evolves on a much faster time scale than the classical variables. Traditional methods cannot avoid resolving these oscillations by many tiny time steps and with huge computational effort. In this article it is shown how the same accuracy can be obtained with a much larger step size. After a transformation of the problem to a numerically more suitable set of equations we construct a new integrator that takes into account the two-scale nature of the system by using an averaging technique for the oscillatory degrees of freedom. We prove that the method remains stable when a large step size is used and show error bounds for the approximations. The efficiency of the integrator is demonstrated in a simple test example.

Mathematics Subject Classification (1991): 65L05, 65L70, 65L20, 65M20, 81-04, 81-08

Key words Oscillatory problem – multiple time scales – numerical integrator – long time steps – error bounds – stability – quantum-classical molecular dynamics – mean field – Ehrenfest model.

1 Introduction

In quantum mechanics the state of a molecular system at time t is represented by a wave function $\Psi = \Psi(t, x, y)$ that depends on the coordinates of the electrons and nuclei denoted by $x \in \mathbb{R}^n$ and $y \in \mathbb{R}^d$, respectively. The time evolution of Ψ follows the *molecular Schrödinger equation*

$$i \varepsilon \partial_t \Psi(t, x, y) = \left(-\frac{\varepsilon^2}{2} \Delta_y + \mathcal{H}_{el}(y) \right) \Psi(t, x, y), \quad (1)$$

where $\mathcal{H}_{el}(y) = -\frac{1}{2} \Delta_x + V(x, y)$ is the electronic Hamilton operator with potential V acting on Ψ as a multiplier. The parameter $\varepsilon > 0$ is the square root of the mass ratio: Let m_{el} be the mass of an electron and suppose, in order to simplify matters, that all nuclei have the same mass¹ m_{nuk} ; then ε is defined by $\varepsilon = \sqrt{m_{el}/m_{nuk}}$. Throughout this paper it is assumed that $m_{el} \ll m_{nuk}$ and consequently that ε is a small parameter ($0 < \varepsilon \ll 1$).

Unfortunately, even rather simple molecules contain so many degrees of freedom that solving (1) exceeds the capacity of any computer. For this reason most simulations of molecular dynamics are entirely based on classical Hamilton systems instead of Schrödinger equations, but this inevitably leads to wrong results whenever quantum effects within the molecule cannot be neglected. In order to include the essential quantum behaviour into classical molecular dynamics several mixed quantum-classical models have been proposed in the literature. One of these approaches, known as *mean field*, *Ehrenfest* or *QCMD* (quantum-classical molecular dynamics), reads:

$$\text{(QCMD)} \begin{cases} \ddot{y} = -\left(\psi^* \nabla_y H(y) \psi\right) & (2) \\ i\dot{\psi} = \frac{1}{\varepsilon} H(y) \psi & (3) \end{cases}$$

In this model the nuclei are considered as classical particles moving along a trajectory $t \mapsto y(t)$ according to a Newtonian equation of motion. The electrons, however, remain quantum particles. They are still represented by a wave function $\psi(t)$ and a Schrödinger equation. Here, $H(y)$ corresponds to the operator $\mathcal{H}_{el}(y)$, but we will assume that an appropriate discretisation of space has already been accomplished. Hence, $H(y) \in \mathbb{R}^{N \times N}$ is a real matrix and $y(t) \in \mathbb{R}^d$ and $\psi(t) \in \mathbb{C}^N$ are time dependent vectors ($d, N \in \mathbb{N}$). As before ε^2 stands for the mass ratio.

¹ This assumption can be avoided at the cost of more complicated equations; cf. [12].

Computing the solutions of (QCMD) numerically is not an easy task because the system is composed of two coupled differential equations with solutions evolving *on two different time scales*. Due to the large factor $1/\varepsilon$ in the right-hand side of (3), the wave function $\psi(t)$ oscillates on a fast time scale $\sim \varepsilon$ while the classical positions $y(t)$ only change on a comparatively slow time scale ~ 1 . Solving the Schrödinger equation (3) with a traditional scheme demands a time step size h substantially smaller than the frequency of oscillation ($h \ll \varepsilon$). The Newtonian equation (2) allows for much larger values of h , but even if one is merely interested in the motion of the nuclei it is unavoidable to approximate the wave function, too, because the right-hand side of (2) depends on ψ .

In [4,7,8,13–16] several methods have already been constructed for (QCMD), but in neither of these papers the problem of a small mass ratio is addressed. These schemes still have to resolve the oscillations of the wave function by means of a small step size $h \ll \varepsilon$ and a large number of time steps. In real-life applications, however, this amounts to huge computational costs because evaluations of $H(y)$ are typically very expensive [12]. Thus, the overall computing time could be vastly reduced by an integrator which attains the desired accuracy with a larger step size $h \approx \varepsilon$ or even $h > \varepsilon$. Some progress in this direction was made in [9,11] where efficient integrators for the *electronic* Schrödinger equation

$$i\dot{\psi}(t) = \frac{1}{\varepsilon}H(t)\psi(t) \quad (4)$$

were proposed. With similar techniques we will develop and analyze a long-time-step method for (QCMD) in this article. Since now the Schrödinger equation is coupled to a second differential equation, additional difficulties arise both in the numerics and in its analysis.

The article is organized as follows. In Section 2 the problem is transformed in order to replace the highly oscillatory solution of (3) by a smoother variable $\eta(t)$. Under certain conditions $\eta(t)$ turns out to be an adiabatic invariant of the quantum part, a result known as the quantum adiabatic theorem. Moreover, the transformed variant of (QCMD) is uniformly well posed with respect to ε , which is a considerable advantage over the original system. Section 3 is devoted to the construction of a time-symmetric integrator. Its performance is demonstrated in comparison to a traditional benchmark scheme. The second half of the paper, comprising Section 4 - 6, investigates the error behaviour of the numerics. As a discrete counterpart of the quantum adiabatic theorem, we show in Section 4 that not only the exact solution of the quantum part but also its numerical approximation is an adiabatic invariant. This serves as an important tool for the

proof of global error bounds in Section 5. We prove that even with a large step size $h > \varepsilon$ our method yields an accuracy of $\mathcal{O}(h)$ in the classical variable $y(t)$ and an accuracy of $\mathcal{O}(\varepsilon)$ in the quantum vector $\eta(t)$. The main difficulty is to verify that the method is uniformly stable in spite of the large step size. This part of the proof is deferred to Section 6. The results of the paper are summarized and discussed in the last section.

This article focuses on the analysis of numerical methods, neither on questions related to modelling nor on applications to realistic molecules. In the past, (QCMD) was applied successfully to a number of chemical problems (cf. [5, 12, 15] and references therein), yet it is known to fail in various situations. Since the pros and cons of this model have been pointed out in [2, 3, 6, 12, 15] these issues are not addressed without questioning their importance. Here, (QCMD) is merely considered as a typical example for a coupled system of differential equations with solutions on different time scales, and the author believes that the ideas can be extended to a broader range of problems.

2 Transformation and analysis of the model

2.1 Assumptions

Let $H(y)$ be a real matrix with the following properties:

- (A1) For all $y \in \mathbb{R}^d$, $H(y) \in \mathbb{R}^{N \times N}$ is symmetric ($d, N \in \mathbb{N}$).
- (A2) Evaluations of $H(y)$ and $\nabla_y H(y)$ are computationally costly, but the diagonalization

$$H(y) = Q(y)\Lambda(y)Q(y)^T, \quad \Lambda(y) = \text{diag}(\lambda_k(y))$$

with an orthogonal matrix $Q(y)$ can be obtained with little additional effort.

- (A3) The eigenvalues $\lambda_k(y)$ of $H(y)$ remain separated: There is a lower bound $\delta_{\min} \gg \sqrt{\varepsilon} > 0$ such that for any pair $\lambda_k(y)$ and $\lambda_l(y)$ with $k \neq l$

$$|\lambda_k(y) - \lambda_l(y)| \geq \delta_{\min} \tag{5}$$

holds for all $y \in \mathcal{U}$ where $\mathcal{U} \subset \mathbb{R}^d$ denotes an appropriate neighborhood of the solution trajectory $\{y(t) \mid t \in [t_0, t_{\text{end}}]\}$.

- (A4) The eigendecomposition is smooth: The matrices $Q(y)$ and $\Lambda(y)$ are twice continuously differentiable with respect to $y \in \mathcal{U}$ with uniformly bounded derivatives.

Discussion. The assumption (A1) is somewhat reasonable because the symmetry of $H(y)$ is inherited from the operator $\mathcal{H}_{el}(y)$. Evaluations of $H(y)$ are costly since each time $\mathcal{H}_{el}(y)$ has to be projected to a suitable subspace of finite dimension. Typically the size of N is rather moderate because only a limited number of electronic states is considered in quantum-classical models; cf. [15]. Therefore the diagonalization of $H(y)$ is much less expensive than its evaluation.

If the third and fourth assumption are true this is called the *adiabatic* situation. In this case the absolute values of the coefficients of the wave function with respect to the eigenbasis remain almost invariant as will be shown in Section 2.4. Though typically the system evolves adiabatically in most parts of phase space, (A3) and (A4) cannot be taken for granted everywhere: Along some trajectories $t \mapsto y(t)$ two different eigenvalues of $H(y)$ may come very close or even intersect while the corresponding eigenvectors suddenly change in a nonsmooth way. This phenomenon is referred to as the *nonadiabatic* situation. Its implications on the behaviour of the solution will be discussed in Section 3.5.

2.2 Transformation

The factor $1/\varepsilon$ in the Schrödinger equation (3) makes its direct numerical treatment difficult because any approximation error would be amplified by $1/\varepsilon$. In [11] the Schrödinger equation was transformed to a more favourable equation prior to any numerical treatment. The same step shall be carried out now for (QCMD).

Let $y(t)$ and $\psi(t)$ be the (unknown) solutions of (QCMD). Using the eigendecomposition of $H(y)$ a new function $\eta(t)$ can be defined by the unitary transformation

$$\eta(t) = \exp\left(\frac{i}{\varepsilon}\Phi(t)\right) Q(y(t))^T \psi(t) \quad (6)$$

where $\Phi(t)$ is the diagonal matrix containing the integrals over the eigenvalues along the solution trajectory $t \mapsto y(t)$:

$$\Phi(t) = \int_{t_0}^t \Lambda(y(s)) ds, \quad \Phi = \text{diag}(\phi_j).$$

Up to an oscillating phase, $\eta(t)$ is the coefficient vector of $\psi(t)$ with respect to the eigenbasis $Q(y)$. Inserting the above transformation into (QCMD) gives rise to a new pair of coupled differential equations. Using the abbreviations

$$K(y) = Q(y)^T (\nabla_y H(y)) Q(y),$$

$$W(y, \dot{y}) = \left(\frac{d}{dt} Q(y) \right)^T Q(y) = \left(\nabla_y Q(y) \dot{y} \right)^T Q(y)$$

we obtain

$$\text{(tQCMD)} \begin{cases} \ddot{y} = -\eta^* \exp\left(\frac{i}{\varepsilon} \Phi\right) K(y) \exp\left(-\frac{i}{\varepsilon} \Phi\right) \eta, & (7) \\ \dot{\eta} = \exp\left(\frac{i}{\varepsilon} \Phi\right) W(y, \dot{y}) \exp\left(-\frac{i}{\varepsilon} \Phi\right) \eta. & (8) \end{cases}$$

Unfortunately, the factor $1/\varepsilon$ is still present in the transformed system (tQCMD), but now it only appears in the argument of the exponential functions. As a consequence the system oscillates faster and faster for $\varepsilon \rightarrow 0$, but since $\|\exp(\pm i\Phi(t)/\varepsilon)\| = 1$ the derivative of $\eta(t)$ is *uniformly bounded* with respect to ε . From this point of view $\eta(t)$ is smoother than $\psi(t)$.

Before other advantages of (tQCMD) can be discussed we have to go through some technicalities.

2.3 Notation

It is helpful to introduce the symbol \bullet for entrywise multiplication of matrices: If $A = (a_{jk})_{j,k} \in \mathbb{C}^{N \times N}$ and $B = (b_{jk})_{j,k} \in \mathbb{C}^{N \times N}$, then $A \bullet B = (a_{jk} b_{jk})_{j,k} \in \mathbb{C}^{N \times N}$. This is motivated by the observation that, e.g., computing $\exp(i\Phi/\varepsilon) K(y) \exp(-i\Phi/\varepsilon)$ in (7) is equivalent to multiplying the (j, k) -th entry of $K(y)$ with $\exp(i(\phi_j - \phi_k)/\varepsilon)$. Let $E(\Phi) \in \mathbb{C}^{N \times N}$ denote the matrix defined by

$$E(\Phi) = \left(e_{kl}(\Phi) \right)_{k,l}, \quad e_{kl}(\Phi) = \begin{cases} \exp\left(\frac{i}{\varepsilon}(\phi_k - \phi_l)\right) & \text{if } k \neq l, \\ 0 & \text{else.} \end{cases}$$

Then (7) and (8) can be restated as

$$\text{(tQCMD)} \begin{cases} \ddot{y} = -\eta^* \left([E(\Phi) + I] \bullet K(y) \right) \eta, & (9) \\ \dot{\eta} = \left(E(\Phi) \bullet W(y, \dot{y}) \right) \eta. & (10) \end{cases}$$

The matrix-tensor-matrix product in $K(y)$ has to be understood in such a way that the k -th entry of equation (9) reads

$$\ddot{y}_k = -\eta^* \left([E(\Phi) + I] \bullet \left(Q(y)^T \left(\frac{\partial}{\partial y_k} H(y) \right) Q(y) \right) \right) \eta.$$

In the definition of $E(\Phi)$ the diagonal was set to zero for technical reasons. This is corrected by adding an identity matrix to $E(\Phi)$ in (9). In the second equation (10) this is not necessary because $W(y, \dot{y})$ is skew-symmetric and therefore has only zeros as diagonal entries. Finally, we define matrices $D(\Lambda) \in \mathbb{R}^{N \times N}$ and $D^-(\Lambda) \in \mathbb{R}^{N \times N}$ by

$$\begin{aligned} D(\Lambda) &= \left(d_{kl}(\Lambda) \right)_{k,l}, & d_{kl}(\Lambda) &= \lambda_k - \lambda_l, \\ D^-(\Lambda) &= \left(d_{kl}^-(\Lambda) \right)_{k,l}, & d_{kl}^-(\Lambda) &= \begin{cases} (\lambda_k - \lambda_l)^{-1} & \text{if } k \neq l, \\ 0 & \text{else.} \end{cases} \end{aligned}$$

This serves the purpose that many of the calculations carried out entrywise can be written in a more compact form. Two basic rules are

$$\frac{d}{dt} E(\Phi(t)) = \frac{i}{\varepsilon} D(\Lambda(t)) \bullet E(\Phi(t)), \quad (11)$$

$$D^-(\Lambda) \bullet D(\Lambda) \bullet M = M \quad (12)$$

for every matrix $M \in \mathbb{C}^{N \times N}$ with zero diagonal. The definitions of $E(\cdot)$, $D(\cdot)$ and $D^-(\cdot)$ are adapted in the obvious way if Φ or Λ are replaced by any other diagonal matrix.

2.4 The quantum adiabatic theorem

Since the oscillatory behaviour of the quantum part originates from the small parameter ε it is natural to ask what happens to the solutions of (1), (4), or (QCMD) in the so-called adiabatic limit $\varepsilon \rightarrow 0$. This question has found considerable interest; cf. [17]. The limit dynamics of (QCMD) was derived in [3]. This result can be seen as an extension of the quantum adiabatic theorem of Born and Fock [1] for the Schrödinger equation.

Theorem 1 (Quantum adiabatic theorem) *Under the assumptions (A1), (A3), and (A4) there is a constant $C > 0$ such that*

$$\|\eta(t) - \eta_0\| \leq C\varepsilon$$

holds uniformly on compact time intervals $[t_0, t_{end}]$.

For convenience of the reader we restate the short proof given in [11].

Proof. Integrating (3) from t_0 to t yields

$$\eta(t) = \eta(0) + \int_{t_0}^t \left(E(\Phi(s)) \bullet W(y(s), \dot{y}(s)) \right) \eta(s) ds.$$

According to (12) we insert

$$W = \frac{i}{\varepsilon} D(\Lambda) \bullet \frac{\varepsilon}{i} D^-(\Lambda) \bullet W$$

and, using (11), integrate by parts:

$$\begin{aligned} \eta(t) &= \eta(0) + \frac{\varepsilon}{i} \left[\left(E(\Phi(s)) \bullet D^-(\Lambda(s)) \bullet W(y(s), \dot{y}(s)) \right) \eta(s) \right]_0^t \\ &\quad - \frac{\varepsilon}{i} \int_0^t \left(E(\Phi(s)) \bullet \frac{d}{ds} \left(D^-(\Lambda(s)) \bullet W(y(s), \dot{y}(s)) \right) \right) \eta(s) ds \\ &\quad - \frac{\varepsilon}{i} \int_0^t \left(E(\Phi(s)) \bullet D^-(\Lambda(s)) \bullet W(y(s), \dot{y}(s)) \right) \dot{\eta}(s) ds. \end{aligned}$$

This yields the assertion. \blacksquare

The quantum adiabatic theorem provides yet another good reason why the transformation from subsection 2.2 is useful: The new quantum function $\eta(t)$ only varies in a range of $\mathcal{O}(\varepsilon)$. For $\varepsilon \rightarrow 0$ the oscillations frequency increases whereas the amplitude decreases such that $\eta(t)$ converges to a *constant* vector. This is a great advantage over the wave function $\psi(t)$. However, the proof reveals that the adiabatic approximation breaks down if the norm of $W(y(t), \dot{y}(t))$ and/or its derivative gets large or if two different eigenvalues almost coincide.

2.5 Well-posedness of the transformed system

One more benefit of the transformation is related to the question of well-posedness. Though it was proven in [3] that a unique solution (y, ψ) of (QCMD) exists on compact time intervals, one cannot expect (QCMD) to be *uniformly* well-posed because small errors in the initial value $\psi(t_0) = \psi_0$ are multiplied by $1/\varepsilon$ and lead to completely different solutions. The transformed system (tQCMD), however, is not afflicted with this undesirable property as the following theorem states.

Theorem 2 (Uniform well-posedness of (tQCMD)) *Under the assumptions (A1), (A3), and (A4) the transformed system (tQCMD) is uniformly well-posed with respect to ε . Let*

$$y(t, y_0, \dot{y}_0, \eta_0), \quad \dot{y}(t, y_0, \dot{y}_0, \eta_0), \quad \eta(t, y_0, \dot{y}_0, \eta_0)$$

be the solution vectors of (tQCMD) that correspond to the initial values y_0, \dot{y}_0 , and η_0 and denote the derivative of the solution vectors with respect to these initial values by

$$\nabla_0 = \frac{\partial}{\partial(y_0, \dot{y}_0, \eta_0)}.$$

Then there is a constant $C > 0$ such that the bounds

$$\begin{aligned}\|\nabla_{\circ} y(t, y_0, \dot{y}_0, \eta_0)\| &\leq C, \\ \|\nabla_{\circ} \dot{y}(t, y_0, \dot{y}_0, \eta_0)\| &\leq C, \\ \|\nabla_{\circ} \eta(t, y_0, \dot{y}_0, \eta_0)\| &\leq C,\end{aligned}$$

hold for all $t \in [t_0, t_{end}]$ and all $\varepsilon > 0$. The constant C only depends on δ_{\min} from (A3), on the bounds of the derivatives in (A4), and on the length $t_{end} - t_0$ of the time interval.

The proof can be found in [10].

3 A numerical method for (tQCMD)

Taking into account the oscillatory behaviour of $E(\Phi)$ we construct a numerical method for (tQCMD) in this section. Let $t_n = t_0 + nh$ with a fixed step size $h > \varepsilon$. Since the equations are coupled, approximations $y_n \approx y(t_n)$ and $\eta_n \approx \eta(t_n)$ have to be computed in an alternating sequence: $y_{n-1} \rightarrow \eta_{n-1} \rightarrow y_n \rightarrow \eta_n \rightarrow y_{n+1} \rightarrow \eta_{n+1}$ and so on. The algorithm is organized in such a way that y_k is already available when η_k is approximated whereas η_k is still unknown when y_k is calculated. Of course, evaluations of $H(y)$ and $\nabla_y H(y)$ are only possible at positions where $y(t_k)$ has already been approximated. In particular, no additional evaluations “between” y_k and y_{k+1} can be made.

3.1 Classical part

3.1.1 Störmer-Verlet. The most popular scheme for Newtonian equations of motion is probably the Störmer-Verlet method. The underlying idea is, on the one hand, to approximate $\ddot{y}(t)$ by the symmetric difference quotient

$$\ddot{y}(t_n) \approx \frac{y(t_n + h) - 2y(t_n) + y(t_n - h)}{h^2} \quad (13)$$

and, on the other hand, to replace $\ddot{y}(t)$ by the differential equation (9). This yields the scheme

$$y_{n+1} - 2y_n + y_{n-1} = -h^2 \eta_n^* \left([E(\Phi_n) + I] \bullet K(y_n) \right) \eta_n. \quad (14)$$

From (14) a new value $y_{n+1} \approx y(t_{n+1})$ can be obtained if y_{n-1} , y_n and η_n are known from previous steps and $\Phi_n \approx \Phi(y_n)$ is computed by the trapezoidal rule

$$\Phi_{k+1} = \Phi_k + \frac{h}{2} (\Lambda(y_{k+1}) + \Lambda(y_k)). \quad (15)$$

The Störmer-Verlet has been used with great success in classical molecular dynamics as well as in other application areas, but when applied to an oscillatory problem like (t)QCMD its performance is rather poor: In (14) the rapidly oscillating exponential functions contained in $E(\Phi)$ are kept fixed at the midpoint, which does not yield any reasonable approximation unless the step size is significantly smaller than the oscillation frequency ($h \ll \varepsilon$); cf. [8].

3.1.2 Averaging Störmer-Verlet. In our situation it is more appropriate to use the equation

$$y(t_n + h) - 2y(t_n) + y(t_n - h) = h^2 \int_{-1}^1 (1 - |\theta|) \ddot{y}(t_n + \theta h) d\theta \quad (16)$$

instead of the difference quotient (13) as proposed in [8]. After substituting $\ddot{y}(t_n + \theta h)$ by the differential equation (9) the phase matrix $E(\Phi(t + \theta h))$ is approximated using the Taylor expansion

$$\Phi(t_n + \theta h) \approx \Phi(t_n) + \theta h \Lambda(y(t_n)) \quad (17)$$

and the trapezoidal rule (15) whereas $\eta(t_n + \theta h)$ and $K(y(t_n + \theta h))$ are frozen at the midpoint t_n as before. This results in a method that from now on will be named *averaging Störmer-Verlet (aSV)*:

$$\text{aSV} \begin{cases} y_{n+1} = h^2 f_n + 2y_n - y_{n-1}, \\ f_n = -\eta_n^* \left([B(y_n) \bullet E(\Phi_n) + I] \bullet K(y_n) \right) \eta_n, \\ B(y_n) = \int_{-1}^1 (1 - |\theta|) E(\theta h \Lambda(y_n)) d\theta. \end{cases}$$

The efficiency of the method is closely related to the fact that the oscillatory variables contained in the force f_n are *integrated*. This is advantageous because the average of an oscillating function contains “more” information than its rather arbitrary value at a single point. Since the entries of $E(\cdot)$ are exponential functions, the integral can be calculated analytically using integration by parts (cf. Section 3.3).

3.1.3 Reformulation as a one-step method. It is well known that the Störmer-Verlet scheme can be rewritten as a one-step-method. An analogous reformulation may be derived for aSV. By means of the auxiliary variables

$$u_{n+\frac{1}{2}} = \frac{y_{n+1} - y_n}{h}, \quad u_n = \frac{u_{n+\frac{1}{2}} + u_{n-\frac{1}{2}}}{2} = \frac{y_{n+1} - y_{n-1}}{2h},$$

aSV can be restated in equivalent form:

$$u_{n+\frac{1}{2}} = u_n + \frac{h}{2}f_n, \quad y_{n+1} = y_n + hu_{n+\frac{1}{2}}, \quad u_{n+1} = u_{n+\frac{1}{2}} + \frac{h}{2}f_{n+1}.$$

In case of a smooth function $y(t)$, $u_{n+\frac{1}{2}}$ and u_n could have been regarded as approximations to the derivatives $\dot{y}(t_n)$ and $\dot{y}(t_{n+\frac{1}{2}})$. It can be seen from (7), however, that $\ddot{y}(t)$ and higher derivatives oscillate. Hence, the difference quotient gives a reasonable approximation to the derivative only if the step size is smaller than the oscillation frequency ($h < \varepsilon$).

3.1.4 Computing the velocities. If required the velocities $\dot{y}(t_n)$ can be computed separately by substituting

$$\ddot{y}(t + \theta h) \approx -\eta_n^* \left(\left(E(\Phi_n + \theta h \Lambda(y_n)) + I \right) \bullet K(y_n) \right) \eta_n \quad (18)$$

in the formula

$$\dot{y}(t + h) = \dot{y}(t - h) + h \int_{-1}^1 \ddot{y}(t + \theta h) d\theta. \quad (19)$$

As before, the integral is calculated analytically and one obtains

$$\begin{aligned} \dot{y}_{n+1} &= \dot{y}_{n-1} + hg_n, \\ g_n &= -\eta_n^* \left(\int_{-1}^1 \left(E(\Phi_n + \theta h \Lambda(y_n)) + I \right) d\theta \bullet K(y_n) \right) \eta_n. \end{aligned} \quad (20)$$

3.2 Quantum part

The simplest way to approximate $\eta(t_n)$ is to do nothing at all and just keep $\eta_n = \eta_0$ constant at the initial value. At first sight, this “method” may look somewhat crude, but according to the quantum adiabatic theorem it yields an approximation of $\mathcal{O}(\varepsilon)$ in the adiabatic situation. In the nonadiabatic case, however, the quantum motion can diverge considerably from its adiabatic limit, and a more sophisticated approximation of $\eta(t)$ is demanded. This is provided by the integrators presented in [11]. The simplest of these methods is constructed as follows. We integrate (10) from $t_n - h$ to $t_n + h$ and freeze the intermediate values $W(y(t_n + \theta h), \dot{y}(t_n + \theta h))$ and $\eta(t_n + \theta h)$ at t_n :

$$\begin{aligned} \eta(t_n + h) &= \eta(t_n - h) + h \int_{-1}^1 \left(E(\Phi(t_n + \theta h)) \right. \\ &\quad \left. \bullet W(y(t_n), \dot{y}(t_n)) \right) d\theta \eta(t_n) + \mathcal{O}(h^2). \end{aligned} \quad (21)$$

The matrix W is approximated by

$$W(y(t_n), \dot{y}(t_n)) \approx W_n = \frac{1}{2h} \left(Q(y_{n+1}) - Q(y_{n-1}) \right)^T Q(y_n),$$

and with (17) and (15) this leads to the *averaging midpoint rule*² (**amp**) from [11]:

$$\text{amp} \quad \eta_{n+1} = \eta_{n-1} + h \left(E(\Phi_n) \bullet \int_{-1}^1 E(\theta h \Lambda(y_n)) d\theta \bullet W_n \right) \eta_n.$$

Again, the integral can be computed analytically (cf. Section 3.3).

3.3 Algorithm of aSV/amp

The method obtained from combining the two integrators **aSV** and **amp** for the two coupled differential equations (9) and (10) will be referred to as **aSV/amp**. Its algorithm reads:

1. Let $y_n, u_{n-\frac{1}{2}}, \dot{y}_{n-1}, \eta_n, \eta_{n-1}, Q(y_n), Q(y_{n-1}), \Lambda(y_n), \Phi_n, K(y_n)$ be given from the previous steps.
2. Put $B(y_n) = \left(b_{kl}(y_n) \right)_{k,l}$ with $b_{kk} = 1$ and

$$b_{kl}(y_n) = -2 \frac{\cos x_{kl} - 1}{x_{kl}^2} \quad (k \neq l)$$

where $x_{kl} = h(\lambda_k(y_n) - \lambda_l(y_n))/\varepsilon$ and $k, l \in \{1, \dots, N\}$.

3. Compute the classical force:

$$f_n = -\eta_n^* \left(\left[B(y_n) \bullet E(\Phi_n) + I \right] \bullet K(y_n) \right) \eta_n.$$

4. Update the positions:

$$u_{n+\frac{1}{2}} = u_{n-\frac{1}{2}} + h f_n,$$

$$y_{n+1} = y_n + h u_{n+\frac{1}{2}}.$$

5. Evaluate $H(y_{n+1})$ and diagonalize:

$$H(y_{n+1}) = Q(y_{n+1}) \Lambda(y_{n+1}) Q(y_{n+1})^T.$$

Evaluate $\nabla H(y_{n+1})$ and put

$$K(y_{n+1}) = Q(y_{n+1})^T (\nabla H(y_{n+1})) Q(y_{n+1})$$

² In [11] this scheme was simply called “Method 1”.

6. Compute W_n :

$$W_n = \frac{1}{2h} (Q(y_{n+1}) - Q(y_{n-1}))^T Q(y_n).$$

7. Update the phase:

$$\Phi_{n+1} = \Phi_n + \frac{h}{2} (A(y_{n+1}) + A(y_n)).$$

8. Put $A(y_n) = \left(a_{kl}(y_n) \right)_{k,l}$ with $a_{kk} = 0$ and

$$a_{kl}(y_n) = 2 \frac{\sin x_{kl}}{x_{kl}} \quad (k \neq l)$$

with x_{kl} from step 2 and $k, l \in \{1, \dots, N\}$.

9. Update the quantum vector:

$$\eta_{n+1} = \eta_{n-1} + h \left(A(y_n) \bullet E(\Phi_n) \bullet W_n \right) \eta_n.$$

10. Update the wave function:

$$\psi_{n+1} = Q(y_{n+1}) \exp \left(-\frac{i}{\varepsilon} \Phi_{n+1} \right) \eta_{n+1}. \quad (22)$$

11. Optionally: Compute the velocities:

$$g_n = -\eta_n^* \left([E(\Phi_n) \bullet A(y_n) + 2I] \bullet K_n \right) \eta_n,$$

$$\dot{y}_{n+1} = \dot{y}_{n-1} + h g_n.$$

Remarks.

1. Care should be taken that the ordering of the eigenvalues in A remains the same in all time steps and that the diagonalizations of H do not produce artificial sign changes of the eigenvectors (the columns of Q).

2. It can be seen from the algorithm that our methods are extensions of the traditional Störmer-Verlet scheme and the explicit midpoint rule: These methods are recovered if we put $B(y_n) = E(0) + I$ and $A(y_n) = 2E(0)$ in step 3 and 9, respectively. Note that in the limit $(h/\varepsilon) \rightarrow 0$ we have $x_{kl} \rightarrow 0$ and obtain indeed

$$\lim_{x_{kl} \rightarrow 0} b_{kl}(y_n) = -2 \lim_{x_{kl} \rightarrow 0} \frac{\cos x_{kl} - 1}{x_{kl}^2} = 1,$$

$$\lim_{x_{kl} \rightarrow 0} a_{kl}(y_n) = 2 \lim_{x_{kl} \rightarrow 0} \frac{\sin x_{kl}}{x_{kl}} = 2$$

for the off-diagonal elements of $B(y_n)$ and $A(y_n)$.

3.4 Starting step for aSV/amp

For the starting step the equations (16) and (21) are replaced by

$$y(t_1) = y(t_0) + h\dot{y}(t_0) + h^2 \int_0^1 (1-\theta)\ddot{y}(t_0 + \theta h) d\theta,$$

$$\eta(t_1) = \eta(t_0) + h \int_0^1 \left(E(\Phi(t_0 + \theta h)) \bullet W(y(t_0), \dot{y}(t_0)) \right) d\theta \eta(t_0) + \mathcal{O}(h^2)$$

and all operations are carried out *mutatis mutandis*. Since $\Phi_0 = 0$ in the very first step, y_1 and η_1 are approximated by

$$y_1 = y_0 + hu_{\frac{1}{2}}, \quad u_{\frac{1}{2}} = \dot{y}_0 + hf_0,$$

$$f_0 = -\eta_0^* \left(B(y_0) \bullet K(y_0) \right) \eta_0,$$

$$\eta_1 = \eta_0 + h \left(A(y_0) \bullet W_0 \right) \eta_0,$$

$$W_0 = \frac{1}{h} (Q(y_1) - Q(y_0))^T Q(y_0).$$

The entries $b_{kl}(y_0)$ and $a_{kl}(y_0)$ of the matrices $B(y_0)$ and $A(y_n)$, respectively, are now

$$b_{kl}(y_0) = \begin{cases} -\frac{\exp(ix_{kl}) - \exp(0)}{x_{kl}^2} + \frac{i}{x_{kl}} & \text{if } k \neq l, \\ b_{kk} = 1/2 & \text{if } k = l, \end{cases}$$

$$a_{kl}(y_0) = \begin{cases} \frac{\exp(ix_{kl}) - \exp(0)}{ix_{kl}} & \text{if } k \neq l, \\ 0 & \text{if } k = l, \end{cases}$$

where $x_{kl} = h(\lambda_k(y_0) - \lambda_l(y_0))/\varepsilon$.

3.5 Numerical example

In real-life problems the dynamics of the quantum subsystem is characterized by long periods of adiabatic motion of $\eta(t)$ interrupted by sudden nonadiabatic transitions on a scale of $\mathcal{O}(1)$. This behaviour can be exemplified by means of a rather simple test problem where the position vector $y(t) \in \mathbb{R}^d$ is only a scalar valued function (i.e. $d = 1$). We consider the symmetric matrix

$$H(y) = \begin{pmatrix} \frac{1}{2}(y^2 - 1) & \delta & 0 \\ \delta & \exp(1-y) - 1 & y - 1 \\ 0 & y - 1 & -\frac{1}{8}(2y - 3)^2 - 3 \end{pmatrix}$$

with a parameter $\delta > 0$ that allows to switch easily between the adiabatic ($\delta = 1$) and the nonadiabatic ($\delta = 0.1$) situation as we will see. In fact, this particular choice of $H(y)$ is an extension of the Landau-Zener-matrix [18].

For $\varepsilon = 0.01$ solutions of the transformed system (tQCMD) corresponding to $H(y)$ are to be computed on the time interval $[0, 2]$. As initial values we choose $y_0 = 0$, $\dot{y} = 0.5$, and $\eta_0 = (11 - 2i, 3 + 5i, -7 + i)^T / \sqrt{209}$.

Our method **aSV/amp** is compared to a benchmark scheme consisting of a traditional Störmer-Verlet method and the exponential midpoint rule for the classical and the quantum part, respectively:

$$\begin{aligned} y_{n+1} - 2y_n + y_{n-1} &= -h^2 \psi_n^* \nabla H(y_n) \psi_n, \\ \psi_{n+1} &= \exp\left(-\frac{2ih}{\varepsilon} H(y_n)\right) \psi_{n-1}. \end{aligned} \quad (23)$$

Note that (23) does not use the transformation from Section 2.2 and therefore solves (QCMD) instead of (tQCMD). This means in particular that $\eta(t)$ is not approximated.

In addition we try what happens if η_n is not computed with **amp** but replaced by the adiabatic limit. This method is denoted by **aSV/adia**:

$$\mathbf{aSV/adia} \begin{cases} \text{Compute } y_n \text{ with aSV,} \\ \text{keep } \eta_n = \eta_0 \text{ fixed,} \\ \text{compute } \psi_n = Q(y_n) \exp(-i\Phi_n/\varepsilon) \eta_0. \end{cases}$$

Technical aside. For lack of space only the real parts of the complex vectors $\eta(t) \in \mathbb{C}^3$ and $\psi(t) \in \mathbb{C}^3$ can be shown. The omitted plots of the imaginary parts “look very similar”; i.e., the real and the imaginary parts do not differ in their qualitative behaviour.

3.5.1 Adiabatic case. In a first example let $\delta = 1$. The two plots on the left-hand side of Figure 1 show that for this value of δ the eigenvalues $\lambda_k(y)$ remain separated along the exact solution $y(t)$ and the norm of the coupling matrix $W(y(t), \dot{y}(t))$ is rather moderate. According to the quantum adiabatic theorem we expect the quantum vector to vary only within a very small range. This is confirmed by Figure 2 where the real part of the entries of $\eta(t)$ is shown. The small boxes in the pictures on the left-hand side are magnified on the right-hand side. Here, the approximations computed with time step $h = 0.05 = 5\varepsilon$ are included. We observe an absolute error of order $\mathcal{O}(10^{-3})$ which is a quite rough approximation since the range of $\eta(t)$ is of the same magnitude. In fact, **aSV/amp** does not produce considerably better approximations than **aSV/adia**. This may seem

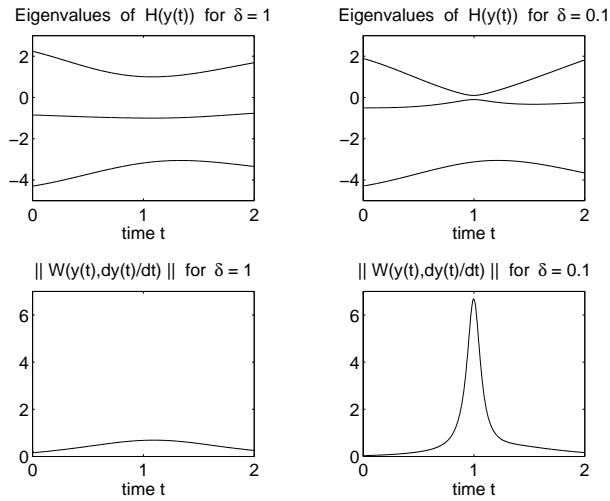


Fig. 1. Eigenvalues $\lambda_k(y(t))$ and norm of the coupling matrix along the exact solution $y(t)$ in the adiabatic case ($\delta = 1$, left-hand side) and in the nonadiabatic case ($\delta = 0.1$, right-hand side).

disappointing at first. Yet, the low precision with respect to η suffices to obtain very satisfying results for ψ as can be seen from Figure 3. In spite of the large step size `aSV/amp` gives excellent approximations to the wave function. This cannot be said about the benchmark scheme (23): It generates more or less “random numbers” with an error of $\mathcal{O}(1)$.

Figure 4 shows the position $y(t)$ and the velocity $\dot{y}(t)$ of the classical degree of freedom. Evidently the benchmark scheme (23) fails when applied with a large step size whereas both `aSV/amp` and `aSV/adia` work with high precision as we observe from the magnifications on the right-hand side.

In the three graphs of Figure 5 the maximum errors on the entire time interval are displayed in logarithmic scale as functions of the step size. For $h \rightarrow 0$ `aSV/amp` exhibits second order convergence in all three components, but the error in $\eta(t)$ only starts to decrease for $h < \varepsilon = 10^{-2}$ and remains almost constant for larger step sizes. Therefore, in all three diagrams `aSV/amp` is only slightly better than `aSV/adia` as long as $h > \varepsilon$. However, both methods clearly achieve a higher accuracy than the benchmark scheme (23) with the same number of matrix evaluations. The difference varies between one and two orders of magnitude (cf. the second and third graph of Figure 5).

In the first example our method definitely outperformed the traditional scheme (23). However, one may ask why the averaging midpoint rule (`amp`) has to be used for the quantum part since for large

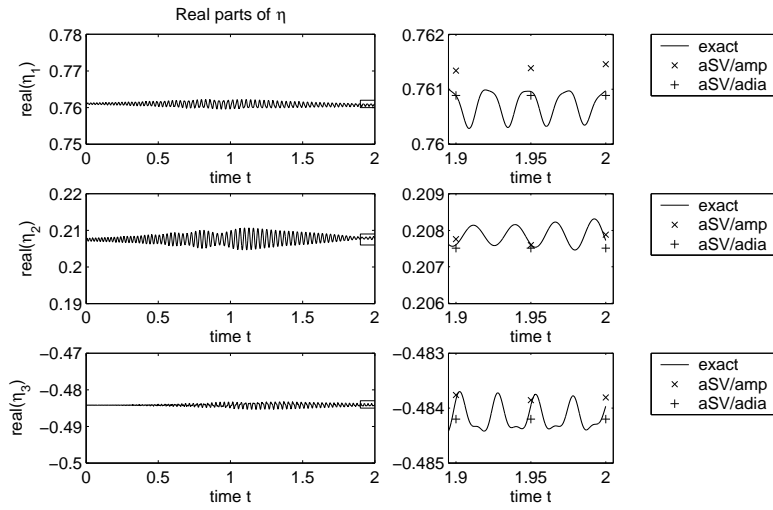


Fig. 2. Left-hand side: Real parts of the exact quantum vector $\eta(t)$ for $\varepsilon = 0.01$ and $\delta = 1$. Right-hand side: Magnification of the areas marked by the boxes. Exact solution and approximations computed with $h = 0.05$.

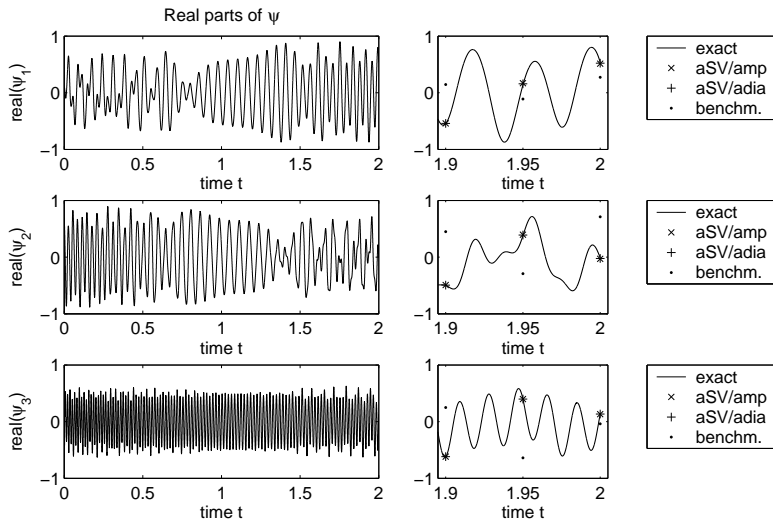


Fig. 3. Left-hand side: Real parts of $\psi(t)$ for $\varepsilon = 0.01$ and $\delta = 1$. Right-hand side: Zoom to end of the time interval. Exact solution and approximations computed with $h = 0.05$.

step sizes it does not yield significantly better approximations than the simple aSV/adia approximation. This question is answered in the second example.

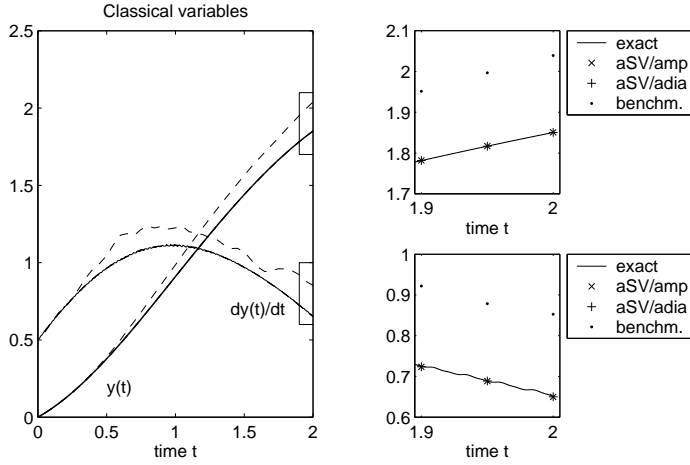


Fig. 4. Classical position and velocity for $\varepsilon = 0.01$ and $\delta = 1$. Exact solution and benchmark scheme (dashed). Right-hand side: Magnification of the areas marked by the boxes. Exact solution and approximations computed with $h = 0.05$.

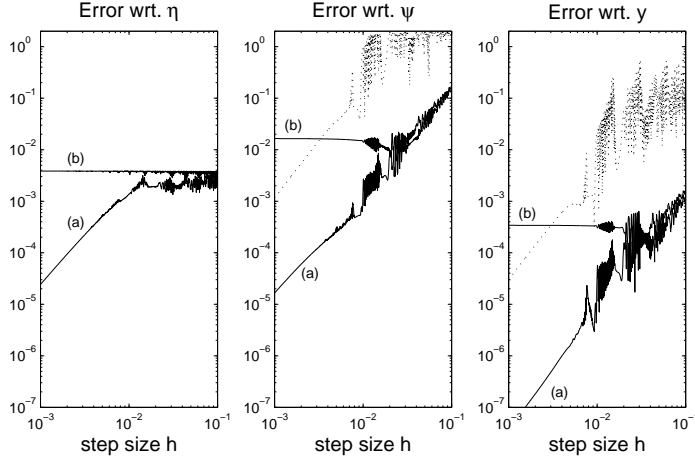


Fig. 5. Maximum error in η , ψ and y as a function of the step size for $\varepsilon = 0.01$ and $\delta = 1$. Logarithmic scale.

3.5.2 Nonadiabatic case. For $\delta = 0.1$ the whole situation changes dramatically. The pictures on the right-hand side of Figure 1 show that the gap between the first two eigenvalues of $H(y(t))$ becomes very small around $t \approx 1$ and that the norm of $W(y(t), \dot{y}(t))$ increases suddenly at the same time. This situation is called *avoided energy level crossing* or *conical intersection* in the literature and is of particular interest in applications. Near an avoided crossing the adiabatic approximation breaks down (cf. the remarks after the proof of The-

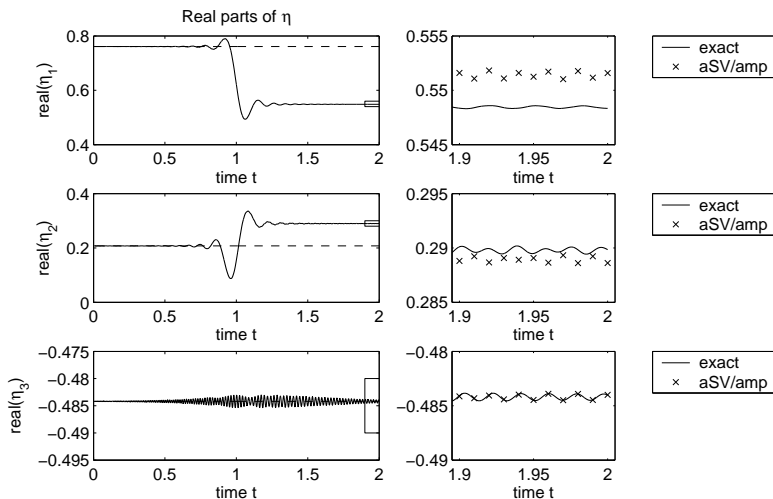


Fig. 6. Left-hand side: Real parts of the exact quantum vector $\eta(t)$ for $\varepsilon = 0.01$ and $\delta = 0.1$. Right-hand side: Magnification of the areas marked by the boxes. Exact solution and approximations computed with $h = 0.01$.

orem 1). Figure 6 shows that around $t \approx 1$ the first two entries of η leave the range of $\mathcal{O}(\varepsilon)$ where they have been oscillating so far and jump to a completely new level. Of course, the multiscale behaviour of the quantum part – small-scale oscillations and a large-scale jump – poses additional difficulties for the numerics. The analysis in [11] reasons that we cannot expect our integrator to give precise results unless we decrease the step size such that $h \ll \delta$. This can be done either by a restart or by an adaptive strategy [11], but in our example we simply choose a fixed step size from the very beginning. For $h = 0.01 = \varepsilon = \delta^2$ `aSV/amp` reproduces the nonadiabatic transition (i.e. the jump on the large scale) quite well though the numerical method ends up on a slightly different level after the avoided crossing than the true solution (cf. right-hand side of Figure 6). The dashed line indicates the constant approximation used in `aSV/adia` which is evidently completely wrong now.

In Figure 7 the entries of $\psi(t)$ are shown. The output of `aSV/adia` is hopelessly bad since it is based on the defective values for $\eta(t)$. The benchmark scheme (23) works a bit better but still suffers from large errors. The best approximation is clearly given by `aSV/amp`. The same holds for the approximation of the classical degrees of freedom (cf. Figure 8).

Figure 9 again shows the relation between the maximum error and the step size. All error curves are smoother than in the previous example since now the main error source is the nonadiabatic transition

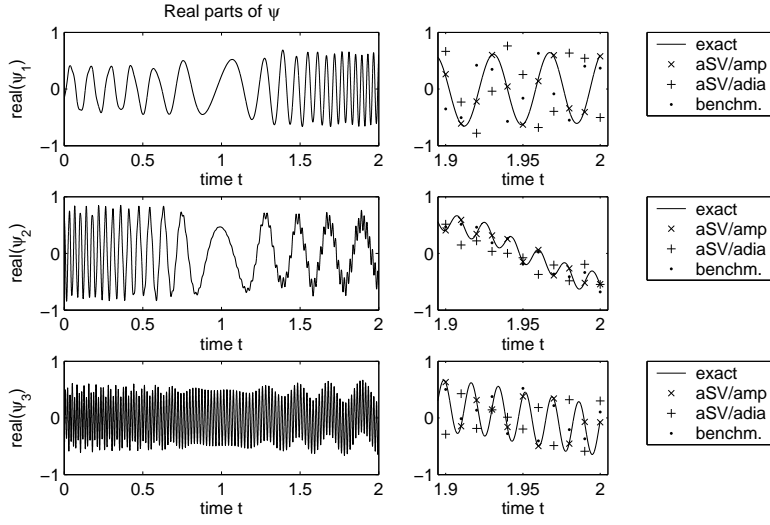


Fig. 7. Left-hand side: Real parts of $\psi(t)$ for $\varepsilon = 0.01$ and $\delta = 0.1$. Right-hand side: Zoom to end of the time interval. Exact solution and approximations computed with $h = 0.01$.

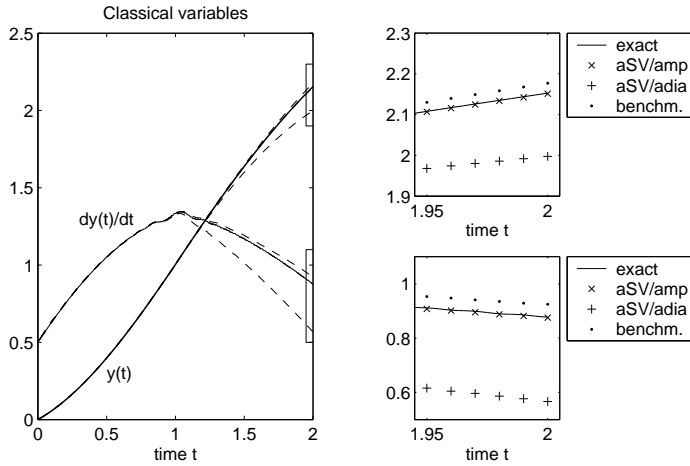


Fig. 8. Classical position and velocity for $\varepsilon = 0.01$ and $\delta = 0.1$. Exact solution and benchmark scheme (dashed). Right-hand side: Magnification of the areas marked by the boxes. Exact solution and approximations computed with $h = 0.01$.

rather than the oscillatory behaviour. For the same reason the error of **aSV/amp** in the η -component starts to decrease even for large step sizes. The improvement achieved with **aSV/amp** in comparison to the benchmark scheme is smaller than in the adiabatic situation and the accuracy is lower than before.

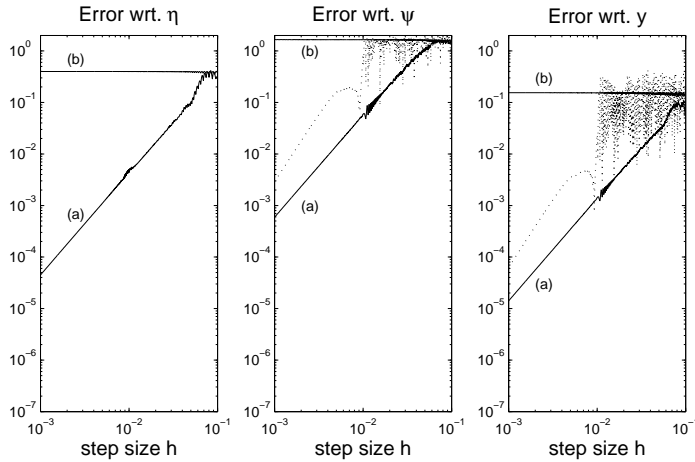


Fig. 9. Maximum error in η , ψ and y as a function of the step size for $\varepsilon = 0.01$ and $\delta = 0.1$. Logarithmic scale.

As a summary of the above examples we find that only the new integrator **aSV/amp** provides good approximations in spite of a relatively large time step. Traditional schemes like (23) fail in the adiabatic situation where the main error is caused by the oscillations of the solution and methods like **aSV/adia** cannot be used whenever nonadiabatic effects occur.

4 A discrete quantum adiabatic theorem

According to the quantum adiabatic theorem $\eta(t)$ stays in a neighborhood of $\mathcal{O}(\varepsilon)$ of the initial value as long as the eigendecomposition of $H(t)$ is smooth and the eigenvalues remain well separated. In this section we prove that this also holds for the approximations η_n .

Proposition 1 (Discrete quantum adiabatic theorem)

Let $0 \leq \varepsilon \ll 1$ and fix $h \leq \sqrt{\varepsilon}$. Under the assumptions (A1)-(A4) from Section 2.1 there is a constant $C > 0$ such that

$$\|\eta_n - \eta_0\| \leq C\varepsilon \quad \forall n = 1, \dots, n_{end}$$

holds for the approximations η_n given by **aSV/amp**. Here and below we put $n_{end} = \max\{n \in \mathbb{N} \mid t_n \in [t_0, t_{end}]\}$.

A remark on notation. For the sake of clearness the abbreviations $K_n = K(y_n)$, $Q_n = Q(y_n)$ and $\Lambda_n = \Lambda(y_n)$ will be used. Note, however, that $\Phi_n \neq \Phi(y_n)$ because Φ_n is defined by the trapezoidal

rule, and that

$$\begin{aligned} W_n &= \frac{1}{2h} \left(Q(y_{n+1}) - Q(y_{n-1}) \right)^T Q(y_n) \\ W_n \neq W(y_n, \dot{y}_n) &= \left(\nabla_{y_n} Q(y_n) \dot{y}_n \right)^T Q(y_n), \\ W_n \neq W(y(t_n), \dot{y}(t_n)) &= \left(\frac{d}{dt} Q(y(t_n)) \right)^T Q(y(t_n)). \end{aligned}$$

Both the diagonal matrix $\Phi \in \mathbb{R}^{N \times N}$ and the vector $(\phi_{11}, \dots, \phi_{NN}) \in \mathbb{R}^N$ containing its diagonal entries are denoted by the same symbol Φ . Since differences of successive Λ_k occur quite often in the formulas below, we put $\Delta_k = \Lambda_k - \Lambda_{k-1}$. Finally, C stands for constants which are not distinguished.

Lemma 1 *Under the assumptions of Proposition 1 the auxiliary variables and the quantum vectors stay bounded, i.e. there is a constant $C > 0$ such that*

$$\|\eta_n\| \leq C, \quad \|u_{n-\frac{1}{2}}\| \leq C, \quad \|y_n - y_{n-1}\| = h \|u_{n-\frac{1}{2}}\| \leq Ch$$

for all $n = 1, \dots, n_{end}$.

Proof of Lemma 1. Rewriting the algorithm as a one-step method yields the recursion

$$\begin{pmatrix} \eta_n \\ \eta_{n-1} \end{pmatrix} = \prod_{j=1}^{n-1} \begin{pmatrix} h \left(A(y_j) \bullet E(\Phi_j) \bullet W_j \right) & I \\ I & 0 \end{pmatrix} \begin{pmatrix} \eta_1 \\ \eta_0 \end{pmatrix}$$

and hence the bound

$$\left\| \begin{pmatrix} \eta_n \\ \eta_{n-1} \end{pmatrix} \right\| \leq \prod_{j=1}^{n-1} (1 + Ch) \left\| \begin{pmatrix} \eta_1 \\ \eta_0 \end{pmatrix} \right\| \leq e^{C(t_{end}-t_0)} \left\| \begin{pmatrix} \eta_1 \\ \eta_0 \end{pmatrix} \right\|$$

for the quantum variables. The boundedness of the auxiliary variables follows from

$$u_{n+\frac{1}{2}} = u_{n-\frac{1}{2}} + hf_n = u_{\frac{1}{2}} + h \sum_{k=1}^n f_k$$

and the fact that the f_k are uniformly bounded. \blacksquare

Lemma 2 *If $M : \mathbb{R}^d \rightarrow \mathbb{R}^{N \times N}$ is a matrix-valued C^2 -function with $\max_y \|\nabla M(y)\| \leq C$ and $\max_y \|\nabla^2 M(y)\| \leq C$, then*

$$\|M(y_{n+1}) - 2M(y_n) + M(y_{n-1})\| \leq Ch^2. \quad (24)$$

Proof of Lemma 2. Let p be the interpolation polynomial through $p(1) = y_{n+1}$, $p(0) = y_n$ and $p(-1) = y_{n-1}$:

$$p(s) = y_{n+1} + (s-1)(y_{n+1} - y_n) + \frac{1}{2}s(s-1)(y_{n+1} - 2y_n + y_{n-1}),$$

$$p'(s) = \frac{1}{2}(y_{n+1} - y_{n-1}) + s(y_{n+1} - 2y_n + y_{n-1}),$$

$$p''(s) = y_{n+1} - 2y_n + y_{n-1}.$$

The bound (24) follows from the equation

$$M(y_{n+1}) - 2M(y_n) + M(y_{n-1}) = \int_{-1}^1 (1 - |s|) \frac{d^2}{ds^2} M(p(s)) ds$$

by applying the chain rule, because

$$\max_{|s| \leq 1} \|p'(s)\| \leq Ch, \quad \max_{|s| \leq 1} \|p''(s)\| \leq Ch^2$$

according to Lemma 1 and by construction of **aSV**, respectively. ■

Proof of Proposition 1. It is sufficient to consider an even number $n \in 2\mathbb{N}$ and prove the estimates

$$\|\eta_{n+1} - \eta_1\| \leq C\varepsilon, \quad \|\eta_1 - \eta_0\| \leq C\varepsilon, \quad \|\eta_n - \eta_0\| \leq C\varepsilon. \quad (25)$$

The η_k follow the recursion

$$\eta_{n+1} - \eta_1 = h\mathcal{A}_n\eta_n + \eta_{n-1} - \eta_1 = h \sum_{k=1}^{n/2} \mathcal{A}_{2k}\eta_{2k} \quad (26)$$

with the matrix

$$\begin{aligned} \mathcal{A}_{2k} &= A(y_{2k}) \bullet E(\Phi_{2k}) \bullet W_{2k} \\ &= E(\Phi_{2k}) \bullet \left(\frac{\varepsilon}{i\hbar} D^-(\Lambda_{2k}) \right) \bullet [E(h\Lambda_{2k}) - E(-h\Lambda_{2k})] \bullet W_{2k}. \end{aligned} \quad (27)$$

Since the Φ_{2k} are obtained from the trapezoidal rule (15) we can rearrange

$$\begin{aligned} \Phi_{2k} + h\Lambda_{2k} &= \Phi_{2k+1} - \frac{h}{2}\Delta_{2k+1}, \\ \Phi_{2k} - h\Lambda_{2k} &= \Phi_{2k-1} - \frac{h}{2}\Delta_{2k}, \end{aligned} \quad (28)$$

where $\Delta_j = A_j - A_{j-1}$. In terms of the exponential matrices, this means that

$$\begin{aligned} &E(\Phi_{2k}) \bullet \left(E(h\Lambda_{2k}) - E(-h\Lambda_{2k}) \right) \\ &= E(\Phi_{2k+1}) \bullet E\left(-\frac{h}{2}\Delta_{2k+1}\right) - E(\Phi_{2k-1}) \bullet E\left(-\frac{h}{2}\Delta_{2k}\right). \end{aligned}$$

We substitute this via (27) in (26) and reorder the sum with respect to the indices of $E(\Phi_k)$:

$$\begin{aligned} \eta_{n+1} - \eta_1 &= \frac{\varepsilon}{i} \sum_{k=1}^{n/2} \left(D^-(\Lambda_{2k}) \bullet \left[E(\Phi_{2k+1}) \bullet E\left(-\frac{h}{2}\Delta_{2k+1}\right) \right. \right. \\ &\quad \left. \left. - E(\Phi_{2k-1}) \bullet E\left(-\frac{h}{2}\Delta_{2k}\right) \right] \bullet W_{2k} \right) \eta_{2k} \\ &= \frac{\varepsilon}{i} \sum_{k=1}^{n/2} \left[\left(D^-(\Lambda_{2k-2}) \bullet E(\Phi_{2k-1}) \bullet E\left(-\frac{h}{2}\Delta_{2k-1}\right) \bullet W_{2k-2} \right) \eta_{2k-2} \right. \\ &\quad \left. - \left(D^-(\Lambda_{2k}) \bullet E(\Phi_{2k-1}) \bullet E\left(-\frac{h}{2}\Delta_{2k}\right) \bullet W_{2k} \right) \eta_{2k} \right] \end{aligned} \quad (29)$$

$$+ \frac{\varepsilon}{i} \left(D^-(\Lambda_n) \bullet E(\Phi_{n+1}) \bullet E\left(-\frac{h}{2}\Delta_{n+1}\right) \bullet W_n \right) \eta_n \quad (30)$$

$$- \frac{\varepsilon}{i} \left(D^-(\Lambda_0) \bullet E(\Phi_1) \bullet E\left(-\frac{h}{2}\Delta_1\right) \bullet W_0 \right) \eta_0. \quad (31)$$

Since (30) and (31) are of order $\mathcal{O}(\varepsilon)$, it remains to show that in (29) the sum stays bounded. This is the case if each of the differences under the sum behave like $\mathcal{O}(h)$. With Lemma 1 and 2 we obtain

$$\begin{aligned} \|D^-(\Lambda_{2k}) - D^-(\Lambda_{2k-2})\| &\leq Ch, \\ \|\eta_{2k} - \eta_{2k-2}\| &= h \|\mathcal{A}_{2k-1} \eta_{2k-1}\| \leq Ch, \\ \left\| E\left(-\frac{h}{2}\Delta_{2k}\right) - E\left(-\frac{h}{2}\Delta_{2k-1}\right) \right\| &\leq C \frac{h}{\varepsilon} \| \Lambda_{2k} - 2\Lambda_{2k-1} + \Lambda_{2k-2} \| \\ &\leq C \frac{h^3}{\varepsilon} \leq Ch, \end{aligned}$$

because $h \leq \sqrt{\varepsilon}$ by assumption. The estimate $W_{2k} - W_{2k-2} = \mathcal{O}(h)$ follows from

$$\begin{aligned} W_{2k} - W_{2k-2} &= \frac{1}{2h} (Q_{2k+1} - Q_{2k-1})^T (Q_{2k} - Q_{2k-2}) \\ &\quad + \frac{1}{2h} (Q_{2k+1} - 2Q_{2k-1} + Q_{2k-3})^T Q_{2k-2} \end{aligned}$$

and the preceding lemmata. This proves the first of the three assertions (25). The second and third one can be shown analogously. \blacksquare

5 Error analysis

For $h < \varepsilon$ it is not very difficult to verify the error bounds

$$\begin{aligned}\|\eta(t_n) - \eta_n\| &\leq C \left(\frac{h}{\varepsilon}\right)^2, \\ \|y(t_n) - y_n\| &\leq C \left(\frac{h}{\varepsilon}\right)^2, \\ \|\dot{y}(t_n) - \dot{y}_n\| &\leq C \left(\frac{h}{\varepsilon}\right)^2\end{aligned}$$

for the approximations given by our method. The same estimates can be shown for the classical Störmer-Verlet method and the explicit midpoint rule, respectively. These bounds explain why second order convergence can be observed in Figure 5 as soon as $h < 10^{-2}$. However, they are useless if the step size h is *larger* than ε . Thus, in this section we study how the error of our method behaves for $h \geq \varepsilon$. Only the adiabatic situation will be considered. The main result is the following theorem.

Theorem 3 *Let $0 \leq \varepsilon \ll 1$ and fix h such that $\sqrt{\varepsilon} \geq h \geq \varepsilon$. Under the assumptions (A1)-(A4) from Section 2.1 the error of the approximations η_n and y_n given by aSV/amp is bounded by*

$$\|\eta(t_n) - \eta_n\| \leq C_1 \varepsilon, \quad n = 1, \dots, n_{end}, \quad (32)$$

$$\|y(t_n) - y_n\| \leq C_2 h. \quad (33)$$

The constants C_1 and C_2 depend on δ_{\min} in (A3), on the bounds of the derivatives in (A4), and on the length of the time interval $[t_0, t_{end}]$, but are independent of ε and h .

Remarks. 1. A corresponding estimate for the velocities is presented in Corollary 1.

2. Though Theorem 3 predicts only $y(t_n) - y_n = \mathcal{O}(h)$ for $h > \varepsilon$, in Figure 5 the error seems to be of second order. The author believes, however, that this behaviour is artificial and will not persist in more complicated examples.

Proof. The first estimate (32) follows immediately from the quantum adiabatic theorem (Theorem 1) and its discrete counterpart (Proposition 1) because

$$\|\eta_n - \eta(t_n)\| \leq \|\eta_n - \eta_0\| + \|\eta_0 - \eta(t_n)\| \leq C\varepsilon. \quad (34)$$

In order to prove (33) we have to study how the error $y(t_n) - y_n$ is affected by errors in η and Φ . Therefore, we introduce the vectors

$$v(t_n) = \begin{pmatrix} y(t_n) \\ y(t_{n-1}) \\ \eta(t_n) \\ \eta(t_{n-1}) \\ \Phi(t_n) \end{pmatrix}, \quad v_n = \begin{pmatrix} y_n \\ y_{n-1} \\ \eta_n \\ \eta_{n-1} \\ \Phi_n \end{pmatrix} \in \mathbb{R}^{2d} \times \mathbb{C}^{2N} \times \mathbb{R}^N,$$

and reformulate the coupled two-step methods **aSV/amp** and the trapezoidal rule (15) as one single one-step “meta method” $F(v_n) = v_{n+1}$ with an abstract function F representing the algorithm from section 3.3. In order to study stability, however, it is unavoidable to consider approximations as functions with respect to the initial values:

Definition 1 *Let*

$$F_k^n(v) = \begin{pmatrix} y_n \\ y_{n-1} \\ \eta_n \\ \eta_{n-1} \\ \Phi_n \end{pmatrix} \in \mathbb{R}^{2d} \times \mathbb{C}^{2N} \times \mathbb{R}^N,$$

denote the vector consisting of approximations obtained by starting at time t_k with initial value $v = v_k$ and executing $n - k$ steps with the algorithm outlined in Section 3.3.

By this definition we have $F_k^n(v) = F_j^n(F_k^j(v))$ and $F_n^n(v) = v$. The error accumulation can be written as

$$\begin{aligned} v_n - v(t_n) &= F_1^n(v_1) - F_n^n(v(t_n)) \\ &= F_1^n(v_1) - F_1^n(v(t_1)) + F_1^n(v(t_1)) - F_n^n(v(t_n)) \\ &= F_1^n(v_1) - F_1^n(v(t_1)) + \sum_{k=1}^{n-1} \left(F_k^n(v(t_k)) - F_{k+1}^n(v(t_{k+1})) \right) \\ &= F_1^n(v_1) - F_1^n(v(t_1)) \\ &\quad + \sum_{k=1}^{n-1} \left(F_{k+1}^n(F_k^{k+1}(v(t_k))) - F_{k+1}^n(v(t_{k+1})) \right). \end{aligned} \tag{35}$$

Now we have to show that the method is stable and that the local error is of second order.

Proposition 2 (Stability) *Under the assumptions of Theorem 3 there is a constant C independent of ε and h such that*

$$\begin{aligned} \left\| F_{k+1}^n \left(F_k^{k+1}(v(t_k)) \right) - F_{k+1}^n(v(t_{k+1})) \right\| &\leq C \left\| F_k^{k+1}(v(t_k)) - v(t_{k+1}) \right\|, \\ \left\| F_1^n(v_1) - F_1^n(v(t_1)) \right\| &\leq C \left\| v_1 - v(t_1) \right\| \end{aligned}$$

for all $1 \leq k < n \leq n_{end}$.

To verify stability in spite of large time steps is the most laborious part of the error analysis. Therefore, we postpone the proof of Proposition 2 to Section 6 and proceed with an investigation of the local error.

Proposition 3 (Local error and starting step) *Under the assumptions of Theorem 3 the local error and the error of the starting step are bounded by*

$$\begin{aligned} \left\| F_k^{k+1}(v(t_k)) - v(t_{k+1}) \right\| &\leq Ch^2, \\ \left\| v_1 - v(t_1) \right\| &\leq Ch \end{aligned}$$

with a constant C independent of ε and h .

Proof of Proposition 3. For exact values $\eta_n = \eta(t_n)$, $\eta_{n-1} = \eta(t_{n-1})$, $y_n = y(t_n)$, $y_{n-1} = y(t_{n-1})$ und $\Phi_n = \Phi(t_n)$ equations (16) and aSV show that $y_{n+1} - y(t_{n+1}) = \mathcal{O}(h^2)$. The error in the quantum part can be estimated as in [11]: From

$$\begin{aligned} W(y(t_n + \theta h), \dot{y}(t_n + \theta h)) &= W(y(t_n), \dot{y}(t_n)) + \mathcal{O}(h) \\ W(y(t_n), \dot{y}(t_n)) &= \frac{1}{2h} \left(Q(y(t_{n+1})) - Q(y(t_{n-1})) \right)^T Q(y(t_n)) \\ &\quad + \frac{h}{2} \int_{-1}^1 \int_0^\tau \frac{d^2}{dt^2} Q(y(t_n + \sigma h)) \, d\sigma \, d\tau, \\ W_n &= \frac{1}{2h} \left(Q(y_{n+1}) - Q(y(t_{n-1})) \right)^T Q(y(t_n)) \end{aligned}$$

and $y_{n+1} = y(t_{n+1}) + \mathcal{O}(h^2)$ we obtain

$$\begin{aligned} \eta(t_{n+1}) - \eta_{n+1} &= h \int_{-1}^1 \left(E(\Phi(t_n + \theta h)) \bullet W_n \right) \eta(t_n) \, d\theta \\ &\quad - h \int_{-1}^1 \left(E(\Phi(t_n) + \theta h \Lambda(y(t_n))) \bullet W_n \right) \eta(t_n) \, d\theta + \mathcal{O}(h^2) \end{aligned}$$

with an error depending on no higher derivatives than \ddot{y} . Inserting the Taylor expansion

$$\Phi(t_n + \theta h) = \Phi(t_n) + \theta h \Lambda(y(t_n)) + (\theta h)^2 R(t_n, y, \theta h)$$

and integrating by parts gives

$$\begin{aligned}
& \int_{-1}^1 E(\Phi(t_n + \theta h)) d\theta - \int_{-1}^1 E(\Phi(t_n) + \theta h \Lambda(y(t_n))) d\theta \\
&= E(\Phi(t_n)) \bullet \int_{-1}^1 E(\theta h \Lambda(y(t_n))) \bullet (E((\theta h)^2 R(t_n, y, \theta h)) - E(0)) d\theta \\
&= E(\Phi(t_n)) \bullet \frac{\varepsilon}{i\hbar} \left[D^-(\Lambda(y(t_n))) \bullet E(\theta h \Lambda(y(t_n))) \right. \\
&\quad \left. \bullet (E((\theta h)^2 R(t_n, y, \theta h)) - E(0)) \right]_{-1}^1 \\
&\quad - E(\Phi(t_n)) \bullet \frac{\varepsilon}{i\hbar} \int_{-1}^1 D^-(\Lambda(y(t_n))) \bullet E(\theta h \Lambda(y(t_n))) \\
&\quad \bullet \frac{d}{d\theta} (E((\theta h)^2 R(t_n, y, \theta h)) - E(0)) d\theta \\
&= \mathcal{O}(h), \text{ because}
\end{aligned}$$

$$\begin{aligned}
E((\theta h)^2 R(t_n, y, \theta h)) - E(0) &= \mathcal{O}\left(\frac{h^2}{\varepsilon}\right), \\
\frac{d}{d\theta} (E((\theta h)^2 R(t_n, y, \theta h)) - E(0)) &= \mathcal{O}\left(\frac{h^2}{\varepsilon}\right).
\end{aligned}$$

This yields as desired $\|\eta(t_{n+1}) - \eta_{n+1}\| \leq Ch^2$.

It is well-known that the error of the trapezoidal rule after one step is

$$\left\| \Phi(t_{n+1}) - \Phi(t_n) - \frac{h}{2} (\Lambda(y(t_{n+1})) + \Lambda(y(t_n))) \right\| \leq Ch^3$$

if exact positions y are used. Replacing $y(t_{n+1})$ by the approximated value $y_{n+1} = y(t_{n+1}) + \mathcal{O}(h^2)$ only causes another error of $\mathcal{O}(h^3)$, and thus $\|\Phi(t_{n+1}) - \Phi_{n+1}\| \leq Ch^3$. The error bounds for the starting step can be derived analogously. ■

Together with (35) the Propositions 2 and 3 yield $\|v_n - v(t_n)\| \leq Ch$ and in particular (33). Hence, up to Proposition 2, the proof of Theorem 3 is completed. □

Remark. The estimate $\|v_n - v(t_n)\| \leq Ch$ implies $\|\eta_n - \eta(t_n)\| \leq Ch$, but as long as $\varepsilon \leq h$ the bound (34) is more precise. The reader may wonder why η_n and η_{n-1} had to be included in the definition of v_n although an error estimate is immediately available from the two quantum adiabatic theorems. The reason is that the technical difficulties caused by the coupling between classical and quantum

variables can be handled more easily if all approximated vectors are contained in v_n .

Once Theorem 3 has been proven it is not very difficult to show a corresponding error estimate for the velocities \dot{y}_n .

Corollary 1 *Under the assumptions of Theorem 3 the error of the approximation \dot{y}_n is bounded by*

$$\|\dot{y}(t_n) - \dot{y}_n\| \leq C h \quad \forall n \in \{1, \dots, n_{end}\}.$$

The constant C is independent of ε and h and only depends on δ_{\min} in (A3), on the bounds of the derivatives in (A4), and on the length of the time interval $[t_0, t_{end}]$.

Proof. The velocities are computed additionally in the sense that neither of the values of η_n , y_n , or Φ_n depends on \dot{y}_n . Hence, no complicated recursion has to be considered. It suffices to show that the approximation (18) only causes an error of $\mathcal{O}(h)$ if $\eta_n = \eta(t_n) + \mathcal{O}(\varepsilon)$ and $y_n = y(t_n) + \mathcal{O}(h)$. This can be done by adapting the techniques used above. \blacksquare

6 Stability: Proof of Proposition 2

6.1 Introduction

We have to prove that $\nabla F_j^n(v)$ is uniformly bounded in ε . Because of

$$\begin{aligned} F_j^n(v) - F_j^n(w) &= \int_0^1 \frac{d}{ds} F_j^n(sv + (1-s)w) ds \\ &= \int_0^1 \nabla F_j^n(sv + (1-s)w) ds (v - w) \end{aligned}$$

this yields

$$\|F_j^n(v) - F_j^n(w)\| \leq C \|v - w\|$$

and the assertion of Proposition 2 follows. For the proof it has to be assumed that the ‘‘subvectors’’ $y_j, y_{j-1}, \eta_j, \eta_{j-1}$ of the initial data $v = v_j$ satisfy the conditions

$$y_j - y_{j-1} = \mathcal{O}(h), \quad \eta_j - \eta_{j-1} = \mathcal{O}(h). \quad (36)$$

This makes sense because stability cannot be expected if the starting values are not consistent. In our situation, (36) may be assumed without loss of generality because the difference of approximations after one step or after the starting step is obviously of order $\mathcal{O}(h)$.

Moreover, we can set $j = 1$ by an appropriate renumbering.

Aim for the remainder of this section: For any $1 \leq n \leq n_{end} - 1$, prove the inequality

$$\begin{aligned} & \|\nabla_o y_{n+1}\| + \|\nabla_o \eta_{n+1}\| + \|\nabla_o \Phi_{n+1}\| \\ & \leq C + Ch \sum_{k=1}^{n+1} \left(\|\nabla_o y_k\| + \|\nabla_o \eta_k\| + \|\nabla_o \Phi_k\| \right) \end{aligned} \quad (37)$$

where $\nabla_o = \frac{\partial}{\partial(y_0, \dot{y}_0, \eta_0)}$, as in Section 2.5, denotes the derivative with respect to the initial values. The uniform boundedness of $\nabla F_j^n(v)$ follows from (37) via a discrete Gronwall lemma. The main difficulty arises wherever terms of the type $E(\Phi)$ are derived because this brings about a factor of $1/\varepsilon$ which has to be equalised somehow. This can be done by partial summation, the discrete counterpart of integration by parts.

6.2 Stability of the classical part

We first prove a Gronwall inequality for the auxiliary variables $u_{n+\frac{1}{2}}$ and then deduce the desired equality for the positions y_n . Since $u_{n+\frac{1}{2}} = u_{n-\frac{1}{2}} + hf_n$ holds by definition we can represent

$$u_{n+\frac{1}{2}} = u_{\frac{1}{2}} + h \sum_{k=1}^n f_k, \quad (38)$$

$$\begin{aligned} f_k &= -\eta_k^* \left(\left[B(y_k) \bullet E(\Phi_k) + I \right] \bullet K(y_k) \right) \eta_k \\ B(y_k) &= \int_{-1}^1 (1 - |\theta|) E(\theta h \Lambda(y_k)) d\theta \\ &= \left(\frac{\varepsilon}{i\hbar} D^-(\Lambda_k) \right)^{\bullet 2} \bullet \left(E(h\Lambda_k) - 2E(0) + E(-h\Lambda_k) \right) \end{aligned} \quad (39)$$

By operations similar to (28) the force can be split into three parts $f_k = f_k^{(1)} + f_k^{(2)} + f_k^{(3)}$ with

$$\begin{aligned} f_k^{(1)} &= -\eta_k^* (I \bullet K_k) \eta_k, \\ f_k^{(2)} &= -\eta_k^* \left(\left(\frac{\varepsilon}{i\hbar} D^-(\Lambda_k) \right)^{\bullet 2} \bullet \left[E(\Phi_{k+1}) \bullet \left(E\left(-\frac{\hbar}{2}\Delta_{k+1}\right) - E(0) \right) \right. \right. \\ &\quad \left. \left. + E(\Phi_{k-1}) \bullet \left(E\left(-\frac{\hbar}{2}\Delta_k\right) - E(0) \right) \right] \bullet K_k \right) \eta_k, \\ f_k^{(3)} &= -\eta_k^* \left(\left(\frac{\varepsilon}{i\hbar} D^-(\Lambda_k) \right)^{\bullet 2} \bullet \left[E(\Phi_{k+1}) - 2E(\Phi_k) + E(\Phi_{k-1}) \right] \bullet K_k \right) \eta_k. \end{aligned}$$

The derivative of $f_k^{(1)}$ is bounded by $\|\nabla_{\circ} f_k^{(1)}\| \leq C\|\nabla_{\circ} \eta_k\| + C\|\nabla_{\circ} y_k\|$. For $\nabla_{\circ} f_k^{(2)}$ we obtain

$$\begin{aligned} \left\| \nabla_{\circ} f_k^{(2)} \right\| &\leq C\|\nabla_{\circ} \eta_k\| + C\|\nabla_{\circ} y_k\| \\ &+ C \left(\frac{\varepsilon}{h} \right)^2 \left\| \nabla_{\circ} \left[E(\Phi_{k+1}) \bullet \left(E \left(-\frac{h}{2} \Delta_{k+1} \right) - E(0) \right) \right] \right\| \\ &+ C \left(\frac{\varepsilon}{h} \right)^2 \left\| \nabla_{\circ} \left[E(\Phi_{k-1}) \bullet \left(E \left(-\frac{h}{2} \Delta_k \right) - E(0) \right) \right] \right\|. \end{aligned} \quad (40)$$

The product rule gives

$$\begin{aligned} &\left\| \nabla_{\circ} \left[E(\Phi_{k+1}) \bullet \left(E \left(-\frac{h}{2} \Delta_{k+1} \right) - E(0) \right) \right] \right\| \\ &= \|\nabla_{\circ} E(\Phi_{k+1})\| \cdot \left\| \left(E \left(-\frac{h}{2} \Delta_{k+1} \right) - E(0) \right) \right\| \\ &\quad + \|E(\Phi_{k+1})\| \cdot \left\| \nabla_{\circ} \left(E \left(-\frac{h}{2} \Delta_{k+1} \right) - E(0) \right) \right\| \\ &\leq \frac{C}{\varepsilon} \|\nabla_{\circ} \Phi_{k+1}\| \cdot \frac{h}{\varepsilon} \|\Delta_{k+1}\| + C \frac{h}{\varepsilon} \|\nabla_{\circ} \Delta_{k+1}\| \\ &\leq C \frac{h^2}{\varepsilon^2} \|\nabla_{\circ} \Phi_{k+1}\| + C \frac{h}{\varepsilon} (\|\nabla_{\circ} y_{k+1}\| + \|\nabla_{\circ} y_k\|), \end{aligned}$$

because by Lemma 1

$$\|\Delta_{k+1}\| = \|A_{k+1} - A_k\| \leq C\|y_{k+1} - y_k\| \leq Ch.$$

A corresponding inequality can be derived for the other term in (40).

This yields the desired bound for $\|\nabla_{\circ} f_k^{(2)}\|$.

Next, the sum $h \sum_{k=1}^n \nabla_{\circ} f_k^{(3)}$ is to be estimated. Before taking the derivative the sum is rearranged with respect to the indices of $E(\Phi_k)$ as in the proof of Proposition 1:

$$\begin{aligned} &\frac{\varepsilon^2}{h} \sum_{k=1}^n \eta_k^* \left(D^-(\Lambda_k)^{\bullet 2} \bullet \left[E(\Phi_{k+1}) - 2E(\Phi_k) + E(\Phi_{k-1}) \right] \bullet K_k \right) \eta_k \\ &= \frac{\varepsilon^2}{h} \sum_{k=1}^n \eta_k^* \left(D^-(\Lambda_k)^{\bullet 2} \bullet \left[E(\Phi_{k+1}) - E(\Phi_k) \right] \bullet K_k \right) \eta_k \\ &\quad + \frac{\varepsilon^2}{h} \sum_{k=1}^n \eta_k^* \left(D^-(\Lambda_k)^{\bullet 2} \bullet \left[E(\Phi_{k-1}) - E(\Phi_k) \right] \bullet K_k \right) \eta_k \\ &= \frac{\varepsilon^2}{h} \sum_{k=1}^n \left[\eta_{k-1}^* \left(D^-(\Lambda_{k-1})^{\bullet 2} \bullet E(\Phi_k) \bullet K_{k-1} \right) \eta_{k-1} \right. \\ &\quad \left. + \eta_k^* \left(D^-(\Lambda_k)^{\bullet 2} \bullet E(\Phi_k) \bullet K_k \right) \eta_k \right] \end{aligned} \quad (41)$$

$$\begin{aligned}
& - \eta_k^* \left(D^-(\Lambda_k)^{\bullet 2} \bullet E(\Phi_k) \bullet K_k \right) \eta_k \Big] \\
& + \frac{\varepsilon^2}{h} \eta_n^* \left(D^-(\Lambda_n)^{\bullet 2} \bullet E(\Phi_{n+1}) \bullet K_n \right) \eta_n \tag{42}
\end{aligned}$$

$$- \frac{\varepsilon^2}{h} \eta_0^* \left(D^-(\Lambda_0)^{\bullet 2} \bullet E(\Phi_1) \bullet K_0 \right) \eta_1 \tag{43}$$

$$\begin{aligned}
& + \frac{\varepsilon^2}{h} \sum_{k=1}^n \left[\eta_{k+1}^* \left(D^-(\Lambda_{k+1})^{\bullet 2} \bullet E(\Phi_k) \bullet K_{k+1} \right) \eta_{k+1} \right. \\
& \quad \left. - \eta_k^* \left(D^-(\Lambda_k)^{\bullet 2} \bullet E(\Phi_k) \bullet K_k \right) \eta_k \right] \tag{44}
\end{aligned}$$

$$+ \frac{\varepsilon^2}{h} \eta_1^* \left(D^-(\Lambda_1)^{\bullet 2} \bullet E(\Phi_0) \bullet K_1 \right) \eta_1 \tag{45}$$

$$- \frac{\varepsilon^2}{h} \eta_{n+1}^* \left(D^-(\Lambda_{n+1})^{\bullet 2} \bullet E(\Phi_n) \bullet K_{n+1} \right) \eta_{n+1}. \tag{46}$$

Bounds for the derivative of (42), (43), (45), or (46) can be derived easily. For example, one obtains for (42)

$$\begin{aligned}
& \frac{\varepsilon^2}{h} \left\| \nabla_o \left(\eta_n^* \left(D^-(\Lambda_n)^{\bullet 2} \bullet E(\Phi_{n+1}) \bullet K_n \right) \eta_n \right) \right\| \\
& \leq \frac{\varepsilon^2}{h} C \left(\|\nabla_o \eta_n\| + \|\nabla_o y_n\| + \|\nabla_o \Phi_{n+1}\|/\varepsilon \right) \\
& \leq C\varepsilon \left(\|\nabla_o \eta_n\| + \|\nabla_o y_n\| \right) + C \|\nabla_o \Phi_{n+1}\|.
\end{aligned}$$

In order to estimate the first sum (41) we apply the product rule

$$\begin{aligned}
& \frac{\varepsilon^2}{h} \sum_{k=1}^n \left\| \nabla_o \left[\eta_{k-1}^* \left(D^-(\Lambda_{k-1})^{\bullet 2} \bullet E(\Phi_k) \bullet K_{k-1} \right) \eta_{k-1} \right. \right. \\
& \quad \left. \left. - \eta_k^* \left(D^-(\Lambda_k)^{\bullet 2} \bullet E(\Phi_k) \bullet K_k \right) \eta_k \right] \right\| \\
& \leq \frac{\varepsilon^2}{h} C \sum_{k=1}^n \left(\|\nabla_o y_k\| + \|\nabla_o y_{k-1}\| + \|\nabla_o \eta_k\| + \|\nabla_o \eta_{k-1}\| \right) \\
& \quad + \frac{\varepsilon^2}{h} C \sum_{k=1}^n \left\| \eta_{k-1}^* \left(D^-(\Lambda_{k-1})^{\bullet 2} \bullet \nabla_o E(\Phi_k) \bullet K_{k-1} \right) \eta_{k-1} \right. \\
& \quad \left. - \eta_k^* \left(D^-(\Lambda_k)^{\bullet 2} \bullet \nabla_o E(\Phi_k) \bullet K_k \right) \eta_k \right\|. \tag{47}
\end{aligned}$$

Again we have to cope with the factor $1/\varepsilon$ caused by $\nabla_o E(\Phi_k)$, but since according to Proposition 1 and Lemma 1

$$\begin{aligned}
& \eta_k - \eta_{k-1} = \mathcal{O}(\varepsilon), \\
& D^-(\Lambda_k)^{\bullet 2} - D^-(\Lambda_{k-1})^{\bullet 2} = \mathcal{O}(h), \\
& K_k - K_{k-1} = \mathcal{O}(h),
\end{aligned}$$

the difference under the sum (47) is of $\mathcal{O}(h/\varepsilon)$. Hence, the first sum (41) is bounded by

$$\varepsilon C \sum_{k=1}^n \left(\|\nabla_o y_k\| + \|\nabla_o y_{k-1}\| + \|\nabla_o \eta_k\| + \|\nabla_o \eta_{k-1}\| + \|\nabla_o \Phi_k\| \right).$$

A similar bound can be obtained for the (44), and together this yields the inequality

$$\|\nabla_o u_{n+\frac{1}{2}}\| \leq C + Ch \sum_{k=1}^{n+1} \left(\|\nabla_o y_k\| + \|\nabla_o \eta_k\| + \|\nabla_o \Phi_k\| \right)$$

for the auxiliary variables. The Gronwall inequality

$$\|\nabla_o y_n\| \leq C + Ch \sum_{k=1}^{n+1} \left(\|\nabla_o y_k\| + \|\nabla_o \eta_k\| + \|\nabla_o \Phi_k\| \right) \quad (48)$$

for the positions is an immediate consequence thanks to the representation

$$y_{n+1} = y_1 + h \sum_{k=1}^n u_{k+\frac{1}{2}}.$$

The stability inequality for Φ follows from the trapezoidal rule:

$$\|\nabla_o \Phi_{n+1}\| \leq \|\nabla_o \Phi_1\| + h \sum_{k=1}^{n+1} \|\nabla_o \Lambda_k\| \leq C + Ch \sum_{k=1}^{n+1} \|\nabla_o y_k\|. \quad (49)$$

6.3 Stability of the quantum part

The discrete quantum adiabatic theorem does not give any information about stability, for its assertion is based on fixed initial values y_0 and η_0 . However, the arguments of its proof can be reused to prove stability of the quantum part. Without loss of generality let $n \in 2\mathbb{N}$ be an even number. We return to the equations (29), (30) and (31) and apply the derivative ∇_o to all terms. In case of (30) this leads to

$$\begin{aligned} & \left\| \frac{\varepsilon}{i} \nabla_o \left(D^*(\Lambda_n) \bullet E(\Phi_{n+1}) \bullet E\left(-\frac{h}{2}\Delta_{n+1}\right) \bullet W_n \right) \eta_n \right\| \\ & \leq \varepsilon C \left(\|\nabla_o y_n\| + \|\nabla_o \eta_n\| + \frac{1}{\varepsilon} \|\nabla_o \Phi_{n+1}\| \right. \\ & \quad \left. + \frac{h}{\varepsilon} (\|\nabla_o y_{n+1}\| + \|\nabla_o y_n\|) + \|\nabla_o W_n\| \right). \end{aligned}$$

In order to derive a bound for $\|\nabla_o W_n\|$ we find that

$$\begin{aligned} W_n &= \frac{1}{2h} \int_0^1 \frac{d}{ds} Q(sy_{n+1} + (1-s)y_{n-1})^T ds Q(y_n) \\ &= \frac{1}{2h} \int_0^1 \nabla Q(sy_{n+1} + (1-s)y_{n-1})^T ds (y_{n+1} - y_{n-1}) Q(y_n) \\ &= \frac{1}{2} \int_0^1 \nabla Q(sy_{n+1} + (1-s)y_{n-1})^T ds (u_{n+\frac{1}{2}} + u_{n-\frac{1}{2}}) Q(y_n) \end{aligned}$$

and, with $\frac{1}{h}(y_{n+1} - y_{n-1}) = u_{n+\frac{1}{2}} + u_{n-\frac{1}{2}}$, obtain from the chain rule

$$\begin{aligned} \|\nabla_o W_n\| &\leq C \left\| \max_x \nabla^2 Q(x) \right\| (\|\nabla_o y_{n+1}\| + \|\nabla_o y_{n-1}\|) \\ &\quad + C \|\nabla_o u_{n+\frac{1}{2}}\| + C \|\nabla_o u_{n-\frac{1}{2}}\| + C \|\nabla_o y_n\|. \end{aligned}$$

The stability of the auxiliary variables and (49) now yield

$$\begin{aligned} &\left\| \frac{\varepsilon}{i} \nabla_o \left(D^-(\Lambda_n) \bullet E(\Phi_{n+1}) \bullet E\left(-\frac{h}{2}(\Lambda_{n+1} - \Lambda_n)\right) \bullet W_n \right) \eta_n \right\| \\ &\leq C + Ch \sum_{k=1}^{n+1} (\|\nabla_o y_k\| + \|\nabla_o \eta_k\|) \end{aligned}$$

for the derivative of (30). The derivative of (31) can be estimated without any difficulty. Finally, an appropriate bound for the derivative of (29) has to be shown by equalizing the factors $1/\varepsilon$ originating from $\nabla_o E(\Phi_{2k-1})$ by verifying that the differences between other terms are of $\mathcal{O}(h)$ as it was done in the proof of the discrete adiabatic theorem. In total, this yields the inequality

$$\|\nabla_o \eta_{n+1}\| \leq C + Ch \sum_{k=1}^{n+1} (\|\nabla_o y_k\| + \|\nabla_o \eta_k\| + \|\nabla_o \Phi_k\|) \quad (50)$$

for the quantum part. The three inequalities (48), (50) and (49) prove the assertion (37). This completes the proof of Proposition 2. \blacksquare

7 Summary and discussion

In this article a long-time-step method for quantum-classical molecular dynamics was proposed. It was shown to be advantageous to transform the underlying system of differential equations, but the prize to pay consists in a diagonalization of the Hamiltonian. The time-reversible method constructed for the transformed problem takes into

account the oscillatory behaviour of the system and attains the accuracy of traditional second order schemes with a much larger step size h . This results in a considerable speedup whenever evaluations of the Hamiltonian dominate the computational costs. It was proven that in the adiabatic case the method is uniformly stable with respect to ε . Even when used with a large time step $\varepsilon < h \leq \sqrt{\varepsilon}$ its error is bounded by $const \cdot h$ in the classical positions and $const \cdot \varepsilon$ in the quantum part. For smaller step sizes second order convergence can be shown.

Unfortunately, some problems could not be solved. The whole stability and error analysis is based on the discrete quantum adiabatic theorem. This theorem is not valid near avoided crossings where nonadiabatic transitions occur due to a non-smooth eigenbasis and a small eigenvalue gap. Therefore, no error estimate for the nonadiabatic situation can be given in this paper. Such an estimate would require a more profound understanding of “what actually happens” near an avoided crossing.

Another problem concerns the rather moderate accuracy in the quantum variable. In Figure 5 the error in η only starts to decrease when $h < \varepsilon$. This observation is confirmed by Theorem 3 which states that $\eta(t_n) - \eta_m = \mathcal{O}(\varepsilon)$ as long as $h > \varepsilon$. Of course this is still better than what most traditional schemes have to offer, but a method converging already for $h > \varepsilon$ would be even more desirable. In [9] several integrators with this property were devised for the decoupled quantum equation

$$\dot{\eta}(t) = \left(E(\Phi(t)) \bullet W(t) \right) \eta(t) \quad (51)$$

which arises from a transformation of the Schrödinger equation (4). These integrators are much more accurate than `amp` when applied to (51), but in case of the coupled system (tQCMD) they would only provide an improvement if at the same time `aSV` was replaced by a more accurate method. How to construct such a method for (9) is at present an open question.

Acknowledgement: This work was partly supported by the DFG Priority Program 1095 *Analysis, Modeling and Simulation of Multi-scale Problems*.

References

1. M. Born and V. Fock, *Beweis des Adiabatenatzes*, Z. Phys. 51 (1928), pp. 165-180.

2. F. A. Bornemann, P. Nettesheim, and Ch. Schütte, *Quantum-classical molecular dynamics as an approximation to full quantum dynamics*, J. Chem. Phys., 105 (1996), pp. 1074-1083.
3. F. A. Bornemann and Ch. Schütte, *On the singular limit of the quantum-classical molecular dynamics model*, SIAM J. Appl. Math., 59 (1999), No. 4, pp. 1208-1224.
4. F. A. Bornemann, P. Nettesheim, B. Schmidt, and Ch. Schütte, *An explicit and symplectic integrator for quantum-classical molecular dynamics*, Chem. Phys. Lett., 256 (1996), pp. 581-588.
5. P. Deuffhard, J. Hermans, B. Leimkuhler, A. E. Mark, S. Reich, R. D. Skeel, eds., *Computational molecular dynamics: challenges, methods, ideas*, Lecture Notes in Computational Science and Engineering 4, Springer, Berlin, 1999.
6. N. L. Doltsinis, *Nonadiabatic Dynamics: Mean-Field and Surface Hopping*, in: J. Grotendorst, D. Marx, and A. Muramatsu, eds., *Quantum Simulations of Complex Many-Body Systems: From Theory to Algorithms*, John von Neumann Institute for Computing, Forschungszentrum Jülich, Jülich, 2002, pp. 377-397.
7. M. Hochbruck and Ch. Lubich, *A bunch of time integrators for quantum/classical molecular dynamics*, in [5], 1999, pp. 421-432.
8. M. Hochbruck and Ch. Lubich, *Exponential integrators for quantum-classical molecular dynamics*, BIT, 39 (1999), No. 4, pp. 620-645.
9. T. Jahnke, *Long-time-step integrators for almost-adiabatic quantum dynamics*, accepted for publication in SIAM J. Sci. Comput., 2004.
10. T. Jahnke, *Numerische Verfahren für fast adiabatische Quantendynamik*, PhD thesis, Universität Tübingen, Germany, 2003 (in german).
11. T. Jahnke und Ch. Lubich, *Numerical integrators for quantum dynamics close to the adiabatic limit*, Numerische Mathematik 94 (2003), 289-314.
12. D. Marx and J. Hutter, *Ab initio molecular dynamics: Theory and implementation*, in: J. Grotendorst, ed., *Modern methods and algorithms of quantum chemistry*, John von Neumann Institute for Computing, Forschungszentrum Jülich, Jülich, 2000, pp. 329-477.
13. P. Nettesheim and S. Reich, *Symplectic multiple-time-stepping integrators for quantum-classical molecular dynamics*, in [5], 1999, pp. 412-420.
14. P. Nettesheim and Ch. Schütte, *Numerical integrators for quantum-classical molecular dynamics* in [5], 1999, pp. 396-411.
15. P. Nettesheim, *Mixed quantum-classical dynamics: A unified approach to mathematical modelling and numerical simulation*, PhD thesis, Freie Universität Berlin, 2000.
16. S. Reich, *Multiple time scales in classical and quantum-classical molecular dynamics*, J. Comput. Phys. 151, No.1, 49-73 (1999).
17. S. Teufel, *Adiabatic perturbation theory in quantum dynamics*, Lecture Notes in Mathematics 1821, Springer (2003).
18. C. Zener, *Nonadiabatic crossing of energy levels*. Proc. R. Soc London, Ser. A 137 (1932), pp. 696-702.